REU Summer Project 2022: Action potentials in action - Pulse waves in partial differential equations

Author: Florian N. Grün
Supervisor: Prof. Jens D. M. Rademacher

1 Introduction

This work was produced during a short summer internship at Bremen University. Firstly, we look at the standard (non-spatial) *FitzHugh-Nagumo model* given by

$$\begin{aligned} \dot{u}(t) &= -bu(t)(u(t)-1)(u(t)-a) - w(t) + I(t), \\ \dot{w}(t) &= \eta(u(t) - cw(t)), \end{aligned} \tag{FN1}$$

where $\eta, a, b, c > 0, \eta \ll 1$ are real parameters and $I : \mathbb{R} \to \mathbb{R}$ a control impulse. Here we have a 2-dimensional ODE-system which can be analysed numerically rather easily with e.g. `pplane`.

In the second part we investigate the *spatiotemporal FitzHugh-Nagumo model*

$$\begin{aligned} u_t(t,x) &= -bu(t,x)(u(t,x)-1)(u(t,x)-a) - w + \tfrac{1}{L^2}\Delta_x u(t,x), \\ w_t(t,x) &= \eta(u(t,x) - \gamma w(t,x)). \end{aligned} \tag{FN2}$$

Here we employ the software package `pde2path` and focus on numerical computation of branch points and dynamics.

Note directly that for η small, we have one "fast" (u) and one "slow" (w) equation, i.e. changes in w happen slowly, whereas changes in u happen faster; in a u-vs-w plot trajectories move fast horizontally and slow vertically.

1.1 Motivation

In nature, there exist many excitable media, that is a system that is reacting to an impulse with some form of wave. Yet after propagating a wave, the system needs some time to "cool down" before another impulse can be processed and a new wave emitted.

As a vicious example one can think of an wildfire; an impulse (starting a fire at some spot) will cause the fire to spread, but giving another impulse (starting another fire at the same spot) a day late will not do much, first the forest has to regrow before another fire can spread. This time, where the system does not respond to impulses is known as *refraction time*.

Similar processes occur in chemistry (Belousov–Zhabotinsky reaction) and in cardiac and neural systems. An impulse, a rapid rise and fall in the membrane potential of a cell will cause a propagating electric spike (known as *action potential*). After the spike, at entering into the refractory period, the system becomes unresponsive to further excitation, depending of course on the biological components involved.

The more realistic mathematical approach to action potentials in neurons is the 4-dimensional *Hodgkin-Huxley* model, for simplicity and better mathematical understanding we will focus on the 2-dimensional FitzHugh-Nagumo model.

2 The standard FitzHugh-Nagumo model

The aim is to investigate under what parameters and impulses spikes occur in (FN1). Those two terms do not have standardized definitions in the literature, so first we provide our own.

Definition 2.1. *An integrable function $I : \mathbb{R}^+ \to R^+$ is called an **impulse** if it has compact support.*

Definition 2.2. *A trajectory $(u, w) : t \mapsto (u(t), w(t)) \ni \mathbb{R}^2$ with $(u(0), w(0)) = (0, 0)$ has a **spike** at time t_s if $\dot{u}(t_s) > 0$ and $u(t_s) = u_s$ with the spike threshold $u_s := (\sqrt{a^2 - a + 1} + a + 1)/3$.*

Intuitively, we can think of a spike as a trajectory that starts somewhere in the left part, cuts across the spike threshold (red vertical line in Figure 1a) below $\mathcal{N}_{\dot{u}}$, travels once around in a big circle in the u-vs-w phase space and then approaches the stable equilibrium at $(0, 0)$. An impulse causing a spike is strong enough to "transport" the state into a position where it gives a response (i.e. some motion away from the equilibrium, at least for some time). Traveling up and down along the nullcline is very slow, in a u-vs-t plot u we can observe the "spikes" in amplitude ([DP22] Fig. 2.4).

In the following analysis the so called *nullclines* for $I(t) = 0$, i.e. the curves where $\dot{v}$ or $\dot{w}$ are zero, will be crucial. Thus the curves

$$\begin{array}{ll} \mathcal{N}_{\dot{u}}: & w = -bu(u-a)(u-1) =: f(u), \\ \mathcal{N}_{\dot{w}}: & w = \frac{1}{c}u \end{array} \tag{2.1}$$

can have one, two (degenerate) or three intersections depending on the choice of parameters. For large a and b (in fact $(1-a)^2 > 4/(bc)$) there are three intersection points and the system, becomes bistable ([DP22] Fig 2.4e). We are only interested in the case with one intersection, assume thus always that $(1-a)^2 < 4/(bc)$. Moreover as $a > 0$, the equilibrium at $(0, 0)$ is locally stable. Note also that the system is dissipative and all trajectories (even with a spike) will eventually converge to the origin.

2.1 Conditions for spikes

For η small, the flow far away from the $\dot{u}$ nullcline is predominately horizontal. Let the initial condition $(u_0, w_0) = (0, 0)$, the stable equilibrium, and give an impulse $I(t)$ of length T. Once the impulse is finished, it depends on the position of $(v(T), w(t))$ whether the system causes the trajectory to spike or not. For a sketch, see Figure 1. If $(v(T), w(t)) \in A_5$, then clearly the trajectory returns to the origin without any spike. However it is NOT the case (as written in [DP22], Section 2.2.4) that $(v(T), w(t)) \in A_6$ implies a spike. If $(v(T), w(t))$ is in A_6, yet close enough to the $\mathcal{N}_{\dot{u}}$, the trajectory just returns back over the $\mathcal{N}_{\dot{u}}$ and not cross the threshold.

Example 2.3. Take $a = \frac{3}{8}$, $b = 5$, $c = 1$, $\eta = 0.2$ and consider $I(t) = I_0\delta_0(t)$ with $I_0 = \frac{2}{5}$. We show that despite $I_0 > a$, the trajectory will not spike. At $(u, w) = \left(\frac{2}{5}, 0\right)$ we have $(u'(t), w'(t)) = \left(\frac{3}{100}, \frac{2}{25}\right)$, a slope of $\frac{8}{3}$. Define now from $\dot{w} = \frac{8}{3}\dot{u}$ (i.e. $-5u^3 + \frac{55}{8}u^2 - \frac{15}{8}u - w = \frac{3}{40}u - \frac{3}{40}w$),

$$z(u) := \left(\frac{1}{1 - 3/40}\right)\left(-5u^3 + \frac{55}{8}u^2 - \frac{78}{40}u\right). \tag{2.2}$$

Hence for all points $(u(t), w(t)) \in \operatorname{epi} z(u)$ we have $\dot{w} \geq \frac{8}{3}\dot{u}$, the flow is directed steeper upwards than $(\frac{8}{3}, 1)$. Let now $l(u)$ be the line going through the point $(\frac{2}{5}, 0)$, so

$$w(t) \geq \frac{8}{3}u - \frac{16}{15} =: l(u). \tag{2.3}$$

Therefore the intersection between the trajectory (with slope steeper than $\frac{8}{3}$) and $\mathcal{N}_{\dot{u}}$ happens before the intersection of l (with exact slope of $\frac{8}{3}$) and $\mathcal{N}_{\dot{u}}$, which is at $u = 0.421 \ll 0.75 = u_s$ and so the trajectory never crosses the spike threshold.

The next theorem deals with finding an area $A(\eta) \subseteq A_6$ (or the curve describing its left boundary $\partial A(\eta) \cap \mathring{A}_6$) where a spike is guaranteed; intuitively it should hold that $A(\eta) \to A_6$ if $\eta \to 0$.

Theorem 2.4. *Let u_s be the spike threshold, η fixed and define for $\lambda \in \mathbb{R}^+$:*

- *the cubic curve $z_\lambda(u) := \left(\frac{1}{1-c\eta\lambda}\right)(-bu^3 + b(a+1)u^2 - (ba+\eta\lambda)u)$;*
- *the point of intersection between $z_\lambda(u)$ and the vertical line at u_s, i.e. $(u_s, z(u_s))$;*
- *$l_\lambda(u) := \frac{1}{\lambda}u + z(u_s) - \frac{1}{\lambda}u_s$ as the line going through $(u_s, z(u_s))$ with slope $1/\lambda$.*

Let now ($\operatorname{hyp} f := \{(u,r) \in \mathbb{R}\times\mathbb{R} : r \le f(u)\}$)

$$A_\lambda := \{u : a \le u \le u_s\} \cap \operatorname{hyp} l_\lambda \cap \operatorname{hyp} z_\lambda \qquad \text{and} \qquad A(\eta) := \cup_\lambda A_\lambda. \tag{2.4}$$

Then an impulse $I(t)$ starting at time t_0 of length T will cause a spike at time $t_s \ge T$ whenever $(u(t_0+T), w(t_0+T)) \in A(\eta)$.

Proof. Without loss of generality assume that $t_0 = 0$ and let I(t) be an impulse such that $P := (u(T), w(T)) \in A(\eta)$. Then for some $\lambda \in \mathbb{R}^+$, $P \in A_\lambda$ and so $P \in \operatorname{hyp} z_\lambda = \{(u,w) : \dot{u} \ge \lambda\dot{w}\}$, which follows directly from the state equations similar to Example 2.3.

Now the trajectory starting from P always lies below $l_\lambda(u)$, as the flow inside A_λ is directed more rightward than the vector $\left(1, \frac{1}{\lambda}\right)$ (i.e. $(u(t), w(t)) \cdot \left(1, \frac{1}{\lambda}\right) \ge 0$ for any trajectory starting in A_λ) by definition of $\operatorname{hyp} z_\lambda$. However as $|w(u) - z(u)| \ge \varepsilon > 0$ for $u \in [a, u_s]$, the trajectory moves at least at a speed of ε in the u-direction (i.e. there is no point where the flow vanishes) and so reach at some finite time t_s the point $(u(t_s), w(t_s)) = (u_s, w(t))$, a spike occurs. □

Remark 2.5. The converse does not hold. There is positive flux into $A(\eta)$ across $\partial A(\eta) \cap \mathring{A}_6$, e.g. from points in $\operatorname{hyp} z_\lambda \setminus \operatorname{hyp} l_\lambda$ close to l_λ. The "true" boundary could be found by (numerically) finding the trajectory that goes exactly through the point $(u_s, f(u_s))$.

To exactly find the area $A(\eta)$ from the preceding abstract theorem is cumbersome but in some simple cases it is possible to get an exact result.

Remark 2.6. A δ-pulse $I(t) = I_0\delta(t - t_0)$ shifts the state $(u, w) \mapsto (u + I_0, w)$ at time t_0.

Corollary 2.7. *For an impulse of the form $I(t) = I_0\delta(t-t_0)$ to the state $(0, \beta)$, there exists a constant $C_\beta(\eta)$ with $u_s > C_\beta(\eta) > a$ such that any I_0 satisfying $u_s \ge I_0 \ge C_\beta(\eta)$ will cause a spike.*

Proof. Assume implicitly that $\beta < f(u_s)$, otherwise there is no way to end up in $\{u > 0\} \cap \{\dot{u} > 0\}$. Take now $C_\beta(\eta) = \min_u \{A \cap \{(u,w) : w = \beta\}\}$. □

Example 2.8. Let us compute the exact value of $C_0(\eta)$ for the specific set of parameters $a = \frac{3}{8}$, $b = 5$, $c = 1$, $\eta = 0.2$. Now

$$u_s = \frac{3}{4} \quad , \quad z_\lambda(u) = \frac{1}{1-\lambda\eta}\left(-5u^3 + \frac{55}{8}u^2 - \left(\frac{15}{8} + \lambda\eta\right)u\right) \quad , \quad z_\lambda(u_s) = \frac{1}{1-\lambda\eta}\left(\frac{45}{128} - \frac{3\lambda\eta}{4}\right), \tag{2.5}$$

which gives the line

$$l_\lambda(u) = \frac{1}{\lambda}u + \frac{1}{1-\lambda\eta}\left(\frac{45}{128} - \frac{3\lambda\eta}{4}\right) - \frac{3}{4\lambda}. \tag{2.6}$$

Calculate now the roots of $z_\lambda(u)$ (here we only need the second root, $0 = r_1 < r_2 < r_3$) and $l_\lambda(u)$,

$$r_l(\lambda) = \frac{3}{4} - \frac{\lambda}{1-\lambda\eta}\left(\frac{45}{128} - \frac{3\lambda\eta}{4}\right) \quad \text{and} \quad r_z(\lambda) = \frac{11}{16} - \sqrt{\frac{25}{256} - \frac{\lambda\eta}{5}}. \tag{2.7}$$

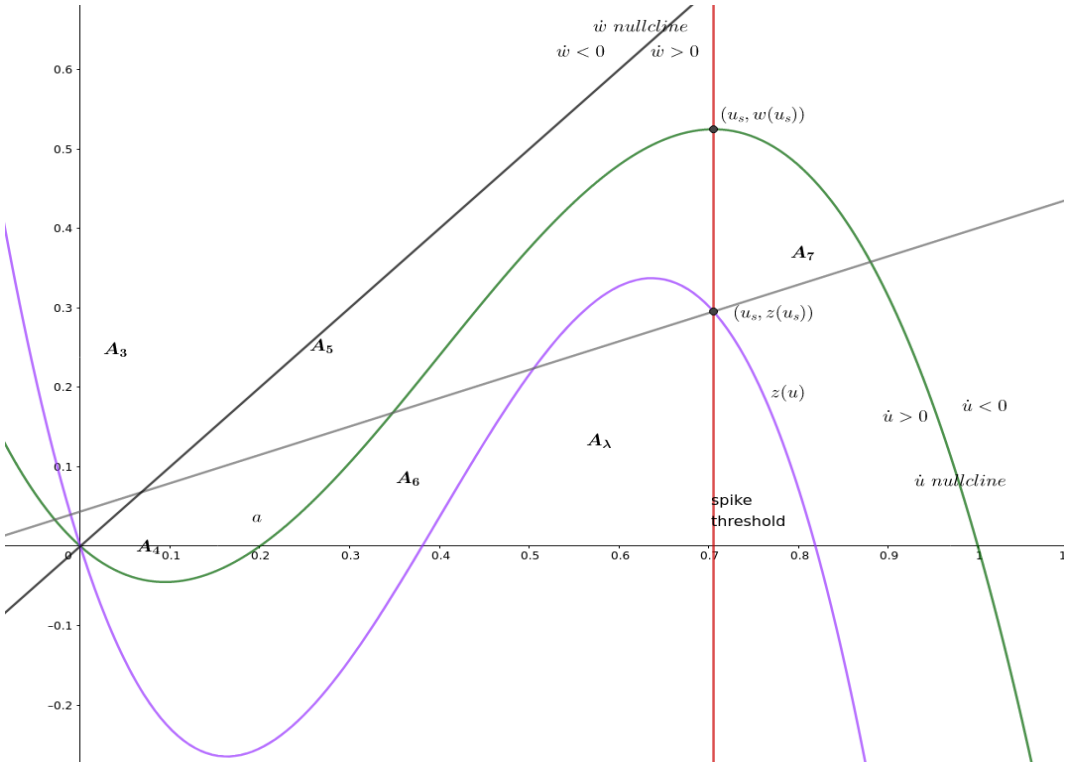

(a) The idea of the proof for Theorem 2.4

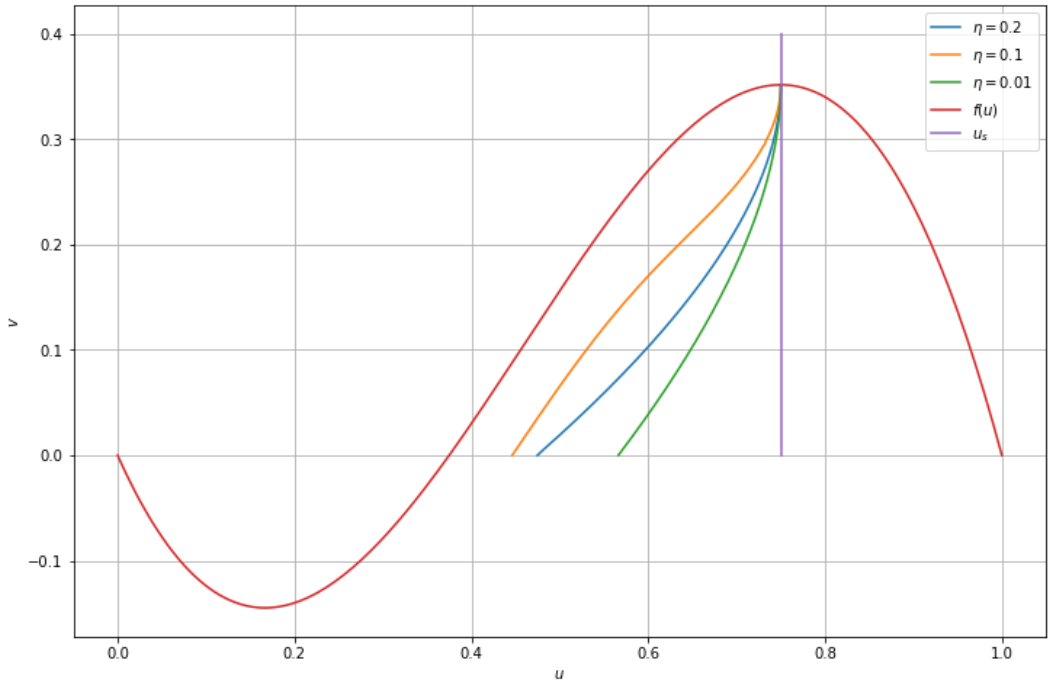

(b) Boundaries for different η, computed numerically

Figure 1: The main setup for the set of parameter values $a = \frac{3}{8}, b = 5, c = 1$

To find $C(\eta)$ solve

$$C_0(\eta) = \min_{\lambda} \max\{r_l(\lambda), r_z(\lambda)\}, \tag{2.8}$$

numerically. *Note that due to the shape of r_l and r_z, if there exist intersections, then the leftmost intersection point is the minimum, otherwise* $\max\{r_l(\lambda), r_z(\lambda)\} = r_l(\lambda)$. *Theoretically, one solves only a quartic polynomial in λ, so there is a closed (but complicated) form for $C_\beta(\eta)$.*

Take now $\eta = 0.2$ and look for solutions to

$$r_l(\lambda) = \frac{3}{4} - \frac{5\lambda}{5-\lambda}\left(\frac{45}{128} - \frac{3\lambda}{20}\right) = \frac{11}{16} - \sqrt{\frac{25}{256} - \frac{\lambda}{25}} = r_z(\lambda) \implies \lambda_* \approx 1.3099, \tag{2.9}$$

which gives

$$C_0(\eta = 0.2) = r_z(\lambda_*) \approx r_z(1.3099) \approx 0.4748. \tag{2.10}$$

Note that for $\eta \to 0$ we have $C_0(\eta) \to a = \frac{3}{8}$ and for $\eta \to \infty$ we have $C_0(\eta) \to \frac{3}{4}$ (see Figure 2), which makes sense intuitively; if $\dot{w} \gg 0$ we need to be close to the spike threshold to "flow over" it.

Remark 2.9. We summarize the general algorithm to find $C_\beta(\eta)$ starting from $(u_0, w_0) = (0, \beta)$ as follows:

1. Calculate the spike threshold u_s.
2. Set up the cubic curve $z_\lambda(u)$.
3. Calculate $z_\lambda(u_s)$ to set up the line $l_\lambda(u) := \frac{1}{\lambda}u + z(u_s) - \frac{1}{\lambda}u_s$.
4. Calculate the $r_l(\lambda)$ as solution of $l_\lambda(u) = \beta$ and $r_u(\lambda)$ as solution of $z_\lambda(u) = \beta$ (take the second intersection).
5. Solve $\min_\lambda \max\{r_l(\lambda), r_z(\lambda)\}$ numerically.

Remark 2.10. The curve $\beta \mapsto (C_\beta(\eta), \beta)$ is equal to $\partial A(\eta) \cap \mathring{A}_6$, the left part of $\partial A(\eta)$. Moreover, for η fixed the function $\beta \mapsto C_\beta(\eta)$ is strictly increasing.

Example 2.11. Using the algorithm outlined in 2.9 we can plot (numerically) the function $\beta \mapsto C_\beta(\eta)$ for $\eta = 0.1$ fixed and the function $\eta \mapsto C_0(\eta)$ for the parameter set $a = \frac{3}{8}, b = 5, c = 1$. As expected both functions are strictly increasing; the former can be seen in Figure 1b, the latter in Figure 2, where we observe the linear relation as $\eta \to 0$.

The next theorem deals with arbitrary impulses, yet general results here are difficult to obtain, due to the coupling and absence of an analytical solution. The impulse needs to be bounded from above to ensure that the trajectory does not travel to far and bounded from below to ensure that it reaches region A. The bounds are really crude and could probably be improved.

Theorem 2.12. *Let $I(t)$ be an impulse of finite length T for* (FN1) *to the steady state* $(0, 0)$ *and* $\beta := T\eta u_s$. *If the following conditions*

(i) $\int_0^T I(t) \le (1 - T^2\eta)u_s - Tf(u_s)$ (upper bound 1),

(ii) $T\eta u_s \le f(u_s)$ (upper bound 2),

(iii) $\int_0^T I(t) \ge \left(1 - \frac{T^2\eta}{1-T^2\eta}\right)^{-1}\left(C_\beta(\eta) + \frac{T^3\eta f(u_s)}{1-T^2\eta} - T\min_{u\in[0,u_s]} f(u)\right)$ (lower bound),

are satisfied, then the trajectory has a spike for some $t_s > T$.

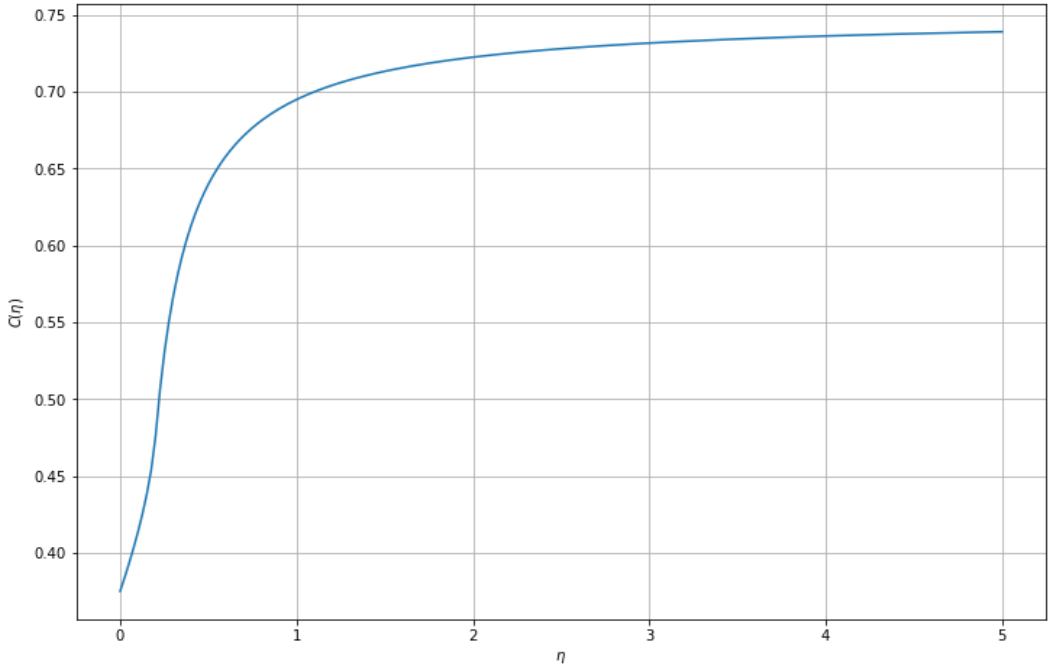

(a) Behaviour for large η

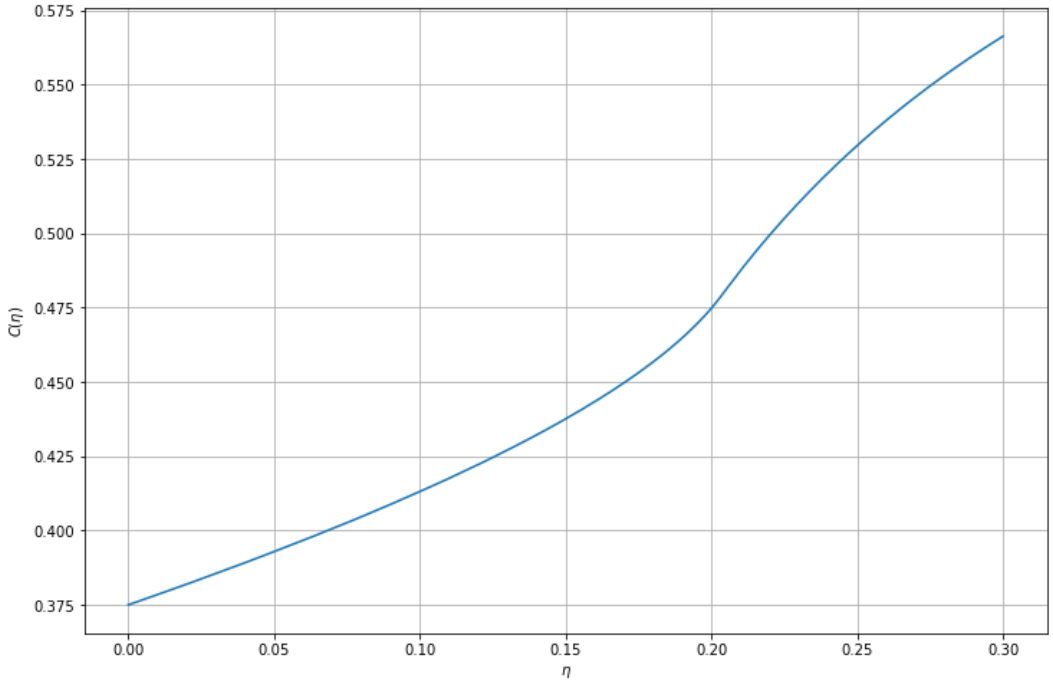

(b) Behaviour for small η

Figure 2: Relation between η and $C_0(\eta)$, computed numerically

Proof. To assure that the impulse does not send the trajectory to far, start by estimating u and w

(use that here $w(t) \geq 0$ for all $t \in [0,T]$),

$$\begin{aligned}
w_m &:= \max_{t\in[0,T]} w(t) = \int_0^{t_m} \eta u(t) - \eta c w(t) \leq \int_0^{t_m} \eta u(t) \leq T\eta u_m, \\
u_m &:= \max_{t\in[0,T]} u(t) = \int_0^{t_m} f(u(t)) - w(t) + I(t) \\
&\leq T \max_{t\in[0,T]} f(u(t)) + \int_0^T I(t) \\
&\leq T \max_{t\in[0,T]} \{w_m, f(u_s)\} + \int_0^T I(t) \\
&\leq T^2\eta u_m + Tf(u_s) + \int_0^T I(t) \\
&\implies u_m \leq \frac{1}{1-T^2\eta}\left(Tf(u_s) + \int_0^T I(t)\right) \leq u_s \qquad \text{from upper bound 1,} \\
&\implies w_m \leq T\eta u_m \leq T\eta u_s \leq f(u_s) \qquad \text{from upper bound 2.}
\end{aligned} \tag{2.11}$$

Hence $u(T) \leq u_s$ and $w(T) \leq f(u_s)$, so it remains to check that $(u(T), w(T))$ is really inside A and under the parabola $f(u)$. Set now $\beta = T\eta u_s$ and compute $C_\beta(\eta)$, then

$$\begin{aligned}
u(T) &= \int_0^T f(u(t)) - \int_0^T w(t) + \int_0^T I(t) \\
&\geq T \min_{u\in[0,u_s]} f(u) - Tw_m + \int_0^T I(t) \\
&\geq T \min_{u\in[0,u_s]} f(u) - T^2\eta u_m + \int_0^T I(t) \\
&\geq T \min_{u\in[0,u_s]} f(u) - \frac{T^3\eta f(u_s)}{1-T^2\eta} + \left(1 - \frac{T^2\eta}{1-T^2\eta}\right)\int_0^T I(t) \\
&\geq C_\beta(\eta) \qquad \text{from the lower bound.}
\end{aligned} \tag{2.12}$$

It is already known that $0 > \min_{u\in[0,u_s]} f(u) = f\left(\frac{a+1-\sqrt{a^2-a+1}}{3}\right) < -\infty$. We conclude that $C_\beta(\eta) \leq u(T) \leq u_s$ and $0 \leq w(T) \leq \beta$ and thereby $(u(T), w(T))$ lies in A so the trajectory will spike at some time $t_s > T$. □

Remark 2.13. Again as $T \to 0$ we recover the conditions for a δ-impulse (i.e. $\beta = 0$), so usually "good" impulses have a high amplitude with small support ($0 < T \ll 1$) to achieve the above bounds. Since $C_\beta(\eta) < u_s$ by construction, we can assure existence of impulses satisfying the conditions; they do not exclude each other if T sufficiently small and $\int_0^T I(t)$ large.

2.2 Qualitative analysis of spike trajectories

After studying the trajectory of spikes close to initial time, we will study what happens when trajectories in (FN1) return to the global fix point at the origin. After crossing the spike threshold, it will cross $\mathcal{N}_{\dot{u}}$ on the right, then loop back go leftwards, cross $\mathcal{N}_{\dot{w}}$ and $\mathcal{N}_{\dot{u}}$ to the left.

Proposition 2.14. *Any spike will approach the origin from the first quadrant below $\mathcal{N}_{\dot{u}}$ and never crosses the u-axis for any finite t.*

Proof. Note first that the flow on $\mathcal{N}_{\dot{u}}$ in the second quadrant is only vertical downwards, any trajectory crosses $\mathcal{N}_{\dot{u}}$ only once. At the equilibrium at the origin are two invariant manifolds tangent to the

eigenspaces spanned by the Jacobian matrix J of the system. The trajectory approaches the origin along the slow manifold $\mathcal{M}_{\text{slow}}$ (the one tangent to the eigenspace of the larger eigenvalue, i.e. $(\sqrt{3209}-67)/16, 1)$) from above. In other words, the trajectory is trapped between $\mathcal{M}_{\text{slow}}$ and $\mathcal{N}_{\dot{u}}$. Moreover, as the flow on the negative u-axis is downward, $\mathcal{M}_{\text{slow}}$ lies in one direction entirely between $\mathcal{N}_{\dot{u}}$ and the u-axis. Hence the incoming trajectory will be squeezed between and $\mathcal{N}_{\dot{u}}$. □

Remark 2.15. As $\eta \to 0$, $\mathcal{M}_{\text{slow}}$ will converge to $\mathcal{N}_{\dot{u}}$ pointwise, by Fenichel theorems.

This enables us to construct a "cycle" (It is a improper to speak of a limit cycle, without injecting energy in each circulation the trajectory onverges to the global fixpoint at the origin, the cycle is artificial.) in the following steps

1. Give a δ-impulse of $I_0 \geq C_0(\eta)$.
2. Wait until the trajectory comes back and intersects the line $w = \beta$ at the point $(u(t_1), \beta)$.
3. Send a δ-impulse of size $u(t_1) + I_1$ with $I_1 \geq C_\beta(\eta)$.
4. Wait again until this trajectory comes back and crosses $y = \beta$ at the point $(u(t_2), \beta)$ send another δ-impulse of size $u(t_2) + I_1$.
5. Repeat step 4 each time the trajectory comes back and crosses $y = \beta$ at the point $(u(t_2), \beta)$.

We have now a loop at height β, where at each circulation we have to inject a δ-pulse of size $u(t_2) + I_1$. The period of the cycle $\tau(I_1)$ is determined implicitly. Note that intuitively for a fixed I_1, when $\beta \to 0$ this period gets larger, $\tau_{I_1}(\beta) \to \infty$. This is due to the fact that the trajectory approaches the origin "monotonically" by Proposition 2.14.

Proposition 2.16. *Let $\beta > 0$ be fixed. Then there exists a (not necessarily unique) δ-impulse of size I_* and a corresponding cycle that minimizes the period. That is $\tau(I_*) \leq \tau(I)$ for any other $I \leq u_s$.*

Proof. This follows from the continuity of τ and the fact that I lies in a compact interval, the interval from the true threshold value $\tilde{C}_\beta(\eta)$ (see Remark 2.5) to u_s. □

2.3 Further perspectives and open questions

A lot remains to be said about the analytical properties of (FN1). Some possible directions are:

- Is there a region $B(\eta) \subset A_5$, such that if $(u(T), w(T)) \in B(\eta)$ after an impulse, it is guaranteed that no spike will occur? So far it is only known that $\partial B(\eta)$ has to lie left of $\tilde{C}(\eta)$.
- Can one calculate e.g. $\tilde{C}_0(\eta)$ through other means then to backtrack the trajectory going through $(u_s, f(u_s))$?
- Can the conditions for arbitrary impulses be improved using more sophisticated estimates?
- Can the bounds for arbitrary impulses be improved by using some regularity of the impulse function $I(t)$?
- Is the minimizing impulse and cycle in Proposition 2.16 unique ?
- Let the size of a δ-impulse be fixed and sufficiently large (not including the first impulse to start the cycle). Calculate the period τ depending on β. Will it decrease as β increases? What is its minimum?
- In what way (linearly, quadratic, etc.) depends the period of a cycle on the parameters a, b, c, η?

3 The spatiotemporal FitzHugh-Nagumo model

In (FN2) u, w are not only functions of time but also of space $u(t,x), w(t,x)$ with $x \in \mathbb{R}^n$ (here $x \in \mathbb{R}^1$). The system is part of the class of *reaction-diffusion models* which are known for pattern formation in space. Instead of a point, the initial condition is now a function $u(0,t) = I_1(x), w(0,t) = I_2(x)$ and it is not possible any longer to observe trajectories and the flow in a phase plot, because $t \mapsto u(t,x)$ maps to a (infinite dimensional function) space.

Analogous to fixed points in non-spatial systems, now we have the so called *uniform steady state*, where $u_t = w_t = 0$ and additionally $u_x = w_x = 0$, in other words u and w are constant. If the uniform state is the only stable solution any initial condition for u and w will either converge to the constant solution or diverge. More interesting behaviour can occur when considering a periodic traveling wave solution, that is a pulse traveling at velocity c in space with time. For instance, a wave travelling in positive x-direction satisfies $u(0,x) = u(t, x+ct)$. For an observer moving parallel with the same velocity, the traveling wave would appear constant and hence $u_t = w_t = 0$, we have eliminated the dependence on t. To do so, perform a change of variable $x = y - ct$ and make the ansatz $u(t,x) = u(t, y-ct)$. Then (FN2) becomes

$$\begin{aligned} 0 \equiv u_t(t,x) &= \frac{1}{L^2} u_{xx}(t,x) + c u_x(t,x) - u(t,x)(u(t,x)-a)(u(t,x)-1) - w(t,x), \\ 0 \equiv w_t(t,x) &= c w_x(t,x) + \eta(u(t,x) - \gamma w(t,x)), \end{aligned} \tag{3.1}$$

which can be rewritten as a first order ODE in $\mathbb{R}^3$.

$$\begin{aligned} u'(x) &= v(x), \\ v'(x) &= -cv(x) + u(x)(u(x)-1)(u(x)-a), \\ w'(x) &= \frac{1}{c}\eta(v(x) - \gamma w(x)). \end{aligned} \tag{3.2}$$

This ODE can be solved numerically, but one has to be careful as the traveling pulse solutions are not stable, nor is the solution unique, so usually the equation is transformed into a boundary value problem and solved with Newtons method. In the following we will use the software `pde2path`, in particular its functions `plotsol(p)`, `cont(p,n)` (stepping along the branch n times with a fixed arc length ds) and `plotbra` which gives the bifurcation branch where a is plotted against $\|\cdot\|_{L^2}$.

3.1 Stability analysis of solution

Let the two solutions in Figure 3 be given.

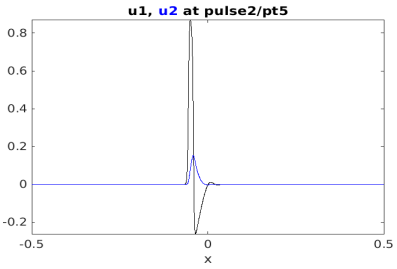

(a) `pt5` with $a = 0.0499273, c = -0.555343, \eta = 0.01, \gamma = 2, L = 1000$

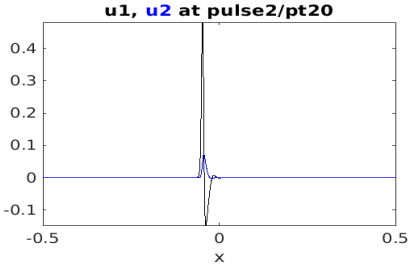

(b) `pt20` with $a = 0.0673935, c = -0.352072, \eta = 0.01, \gamma = 2, L = 1000$

Figure 3: Two different solutions for (3.1), similar in shape but different stability

In both cases we perform a discrete time simulation with n_t time steps of size dt, i.e. study what happens to the solution in (FN2). Stable solutions (e.g. `pt5`) will show a pulse moving to the left

at a constant speed, unstable solutions (e.g. `pt20`) will collapse to zero directly, as they are only a numerical approximation (in form of a finite element/difference solution with n_p elements). We study the stability of `pt5` under perturbations in

(i) the initial data: Will the initial condition `pt5` $+ h$ (h is here a vector of size n_p) converge to `pt5` in the time simulation?

(ii) the parameters: Will `pt5` in the time simulation lead to a stable solution if we perturb the parameters a, c, η, γ or L?

To perturb the initial condition we add normally distributed random noise (with mean 0) to it. Uniformly distributed noise works equally well, yet sufficiently large Gaussian noise can produce opposite moving pulses itself (see Figure 5).

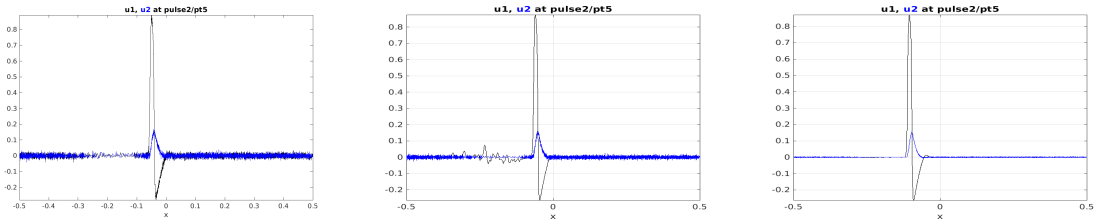

(a) $t = 0$ (b) $t = 20$ (c) $t = 80$

Figure 4: Perturbing initial condition with Gaussian noise with standard deviation $\varepsilon = 0.01$

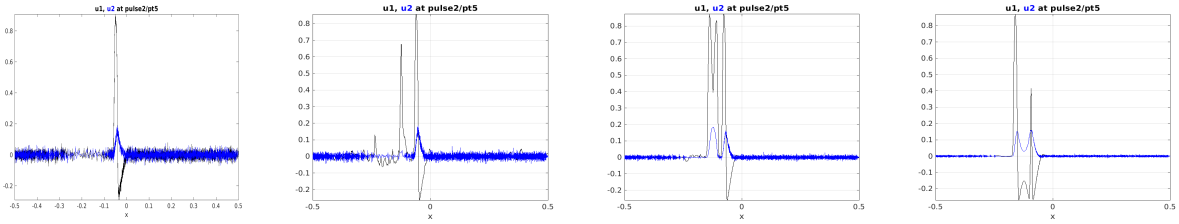

(a) $t = 0$ (b) $t = 20$ (c) $t = 50$ (d) $t = 89$

Figure 5: Perturbing initial condition with Gaussian noise with standard deviation $\varepsilon = 0.02$

When we now perturb the parameters it turns out that all of them are robust (here we mean even up to a perturbation of 50% to a single parameter at a time, the time simulation still gives a traveling pulse). Lastly, we try to find a traveling pulse solution with zero Neumann boundary conditions (i.e. vanishing at the boundary) to a certain set of parameters by starting from a rectangular initial condition. Set $a = 0.05, c = -0.5, \eta = 0.01, \gamma = 2, L = 1000$, in Figure 6 we obtain a traveling pulse, but in any case it is not clear if that is the exact same as `pt5`.

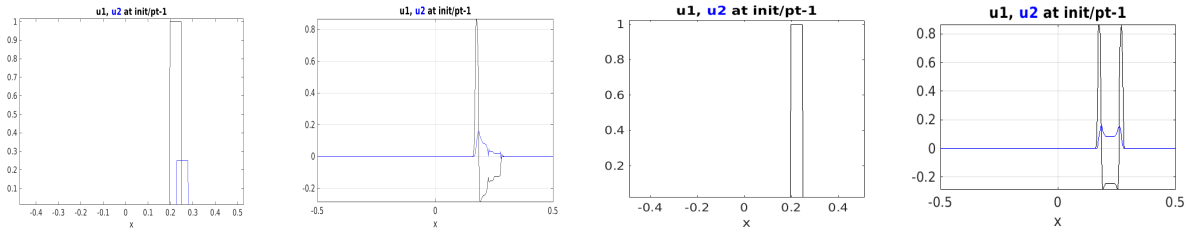

(a) assymetric initial conditions (b) asymetric at $t = 50$ (c) symmetric initial conditions (d) symmetric at $t = 50$, two opposite moving pulses

Figure 6: Time simulation of a traveling pulse initiated by rectangular pulses

3.2 Pulse splitting and Branch jumping

Here we will investigate the behaviour of the "stacked homoclinic bananas" in [CRS21, Chapter 7] using the solution `pt5` instead.

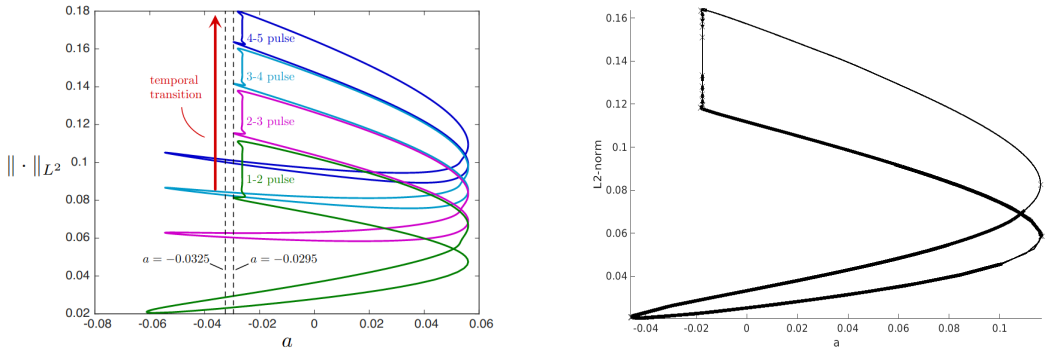

(a) Different homoclinic bananas from [CRS21] (b) The $1-2$ pulse banana

Figure 7: Homoclinic bananas

First investigate the 1-2 branch of our solution `pt5` closer, that is plot its complete bifurcation diagram with stability (Figure 7). Note that the lower parabola represents the 1-pulse solution, the upper one the 2-pulse. There are two transitions (from one pulse to two and vice versa), once in the sharp left turn, once in the straight connecting part with a lot of fold points. We will actually interpolate the solution on a uniform mesh (`pt5` has a finer mesh centered around the spike), in order to not disturb later time simulations and moving pulses too much. Yet the stability diagram of Figure 7b has to be interpreted carefully, actually only the upper part of the 1-pulse parabola is stable under the time simulation. It remains open why the software marks those parts as stable.

Start from the stable 1-pulse `pt5` in counterclockwise direction. After the first fold the 1-pulse becomes unstable, i.e. in the time simulation (we usually use a stepsize of $dt = 0.5$ or $dt = 1$, in some cases too large dt will give instability whereas small dt gives stability) it will die out rather quickly.

After the next fold, closely afterwards, an unstable 2-pulse is expected, yet we observe pulse splitting the emerging of opposite moving pulses (Figure 8). Here we have the exact same number of leftwards and rightwards moving pulses.

Following the path for a bit, the solution turns into the unstable 2-pulse (i.e. dying out of the pulse in the time simulation). The path comes again through a fold point and we observe a "temporarily stable" 2-pulse, that eventually converges to a 1-pulse (Figure 9).

Again a bit further down the path the initial 2-pulse condition converges to another (note the

change in between the two pulses) stable 2-pulse (Figure 10).

Now, for the transition back to the 1-pulse, again pulse splitting occurs, but in two different forms! For solutions "closer" to the 2-pulse parabola, we have a pulse splitting with two more leftwards moving than rightwards moving pulses (Figure 11). Once the path becomes close to connecting back to the stable 1-pulse, there will be only one extra leftwards moving pulse (Figure 12).

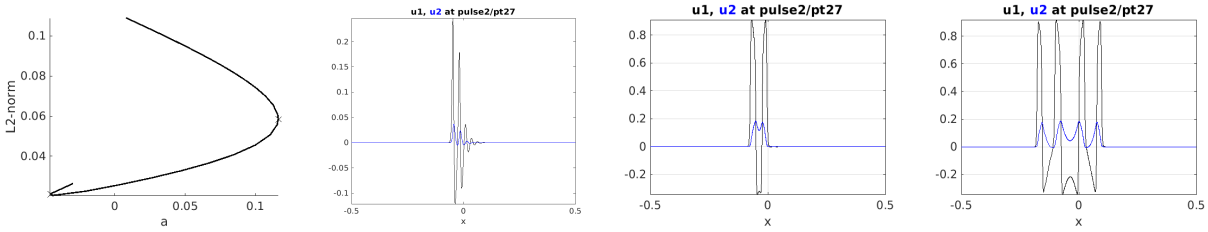

(a) Position in branch (b) $t = 0$ (c) $t = 100$ (d) $t = 200$

Figure 8: Pulse splitting at $a = -0.0296902$, $c = -0.384998$, $\|u\|_{L^2} \approx 0.0264$

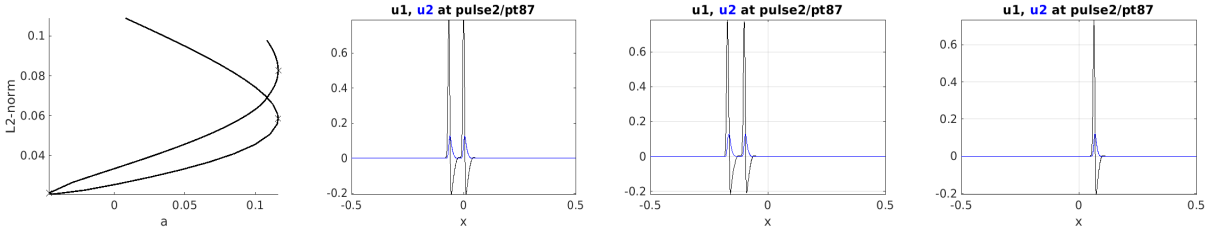

(a) Position in branch (b) $t = 0$ (c) $t = 250$ (d) $t = 5000$

Figure 9: "temporarily stable" 2-pulse at $a = 0.108193$, $c = -0.426884$, $\|u\|_{L^2} \approx 0.0978$

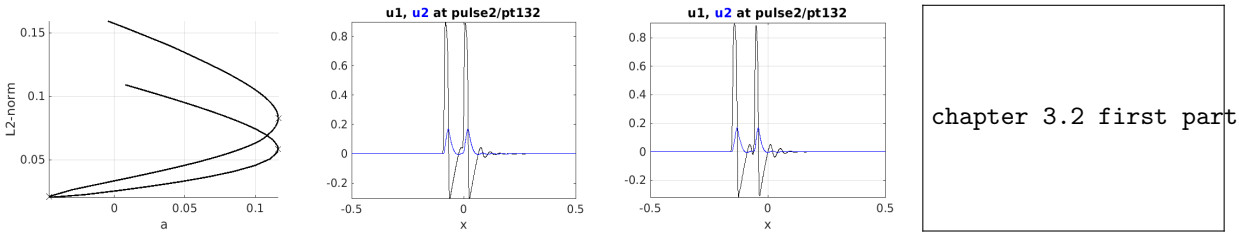

(a) Position in branch (b) $t = 0$ (c) $t = 100$ (d) $t = 300$

Figure 10: Convergence to another stable 2-pulse at $a = -0.00453088$, $c = -0.653619$, $\|u\|_{L^2} \approx 0.159$

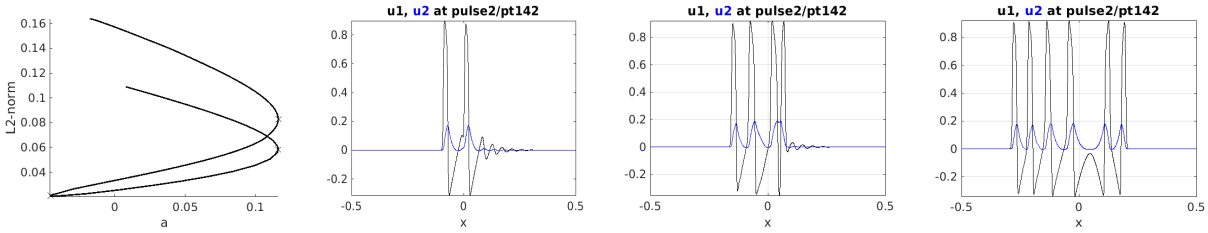

(a) Position in branch (b) $t = 0$ (c) $t = 100$ (d) $t = 300$

Figure 11: Pulse splitting with two extra leftwards moving pulses at $a = -0.0175265$, $c = -0.675396$, $\|u\|_{L^2} \approx 0.163$

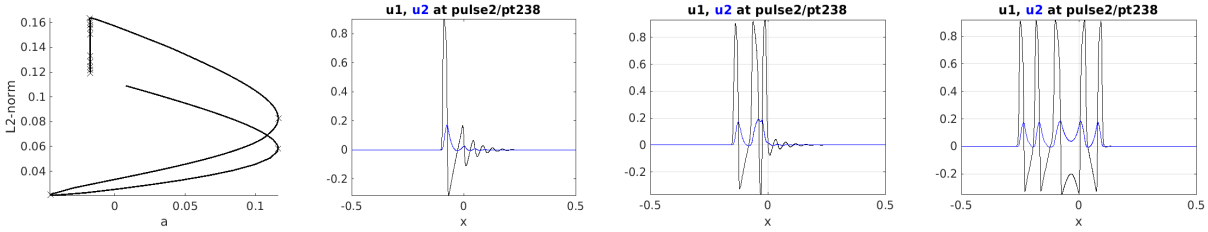

(a) Position in branch (b) $t = 0$ (c) $t = 80$ (d) $t = 250$

Figure 12: Pulse splitting with one extra leftwards moving pulses at $a = -0.0173908$, $c = -0.675175$, $\|u\|_{L^2} \approx 0.119$

Originally, the idea was to start from a solution in the left part of the 1-2 branch, decrease a, perform a time simulation to move upwards in the figure, then increase a again and hope that we land on the 2-3 branch (i.e. when doing the path continuation, trace out the 2-3 branch). However it seems that we either end up with a stable 1-pulse or the setting of Figure 12 and we could not replicate the emerging of single pulses from [CRS21]. Thus we looked for a different way to find the 2-3 (or other higher order) pulse branch.

Well, we already observed a stable 2-pulse in Figure 10. After performing a time simulation (Figure 13), perform now the path continuation with the result of the time simulation.

Remark 3.1. In practice that turned out more difficult than expected, because some stable 2-pulses from the time simulation would not converge in the path continuation. After some playing, we found that exactly 130 steps from `pt5` and a time simulation with $dt = 1$, $nt = 500$ that works as a starting point for an interesting new path continuation. Some other values might lead to totally different paths and branches.

First a third spike will emerge (Figure 13), a time simulation leads to pulse splitting, similar to the transition in the 1-2 branch. Once transitioned to a more "stable" region (without many fold points), the 3-pulse will converge to a stable 3-pulse (Figure 14). (It is not stable itself, note the small change in between the spikes.) The same will occur for a 4-pulse (Figure 15) and eventually for a 5-pulse (Figure 16). Note also that e.g. the 4-pulse resembles a combination of two different 2-pulses, one pair closer to each other the other with a small hump between. It seems that the red branch is not closed like the other higher branches in [CRS21], yet their pulse transitions do resemble the ones in Figure 7.

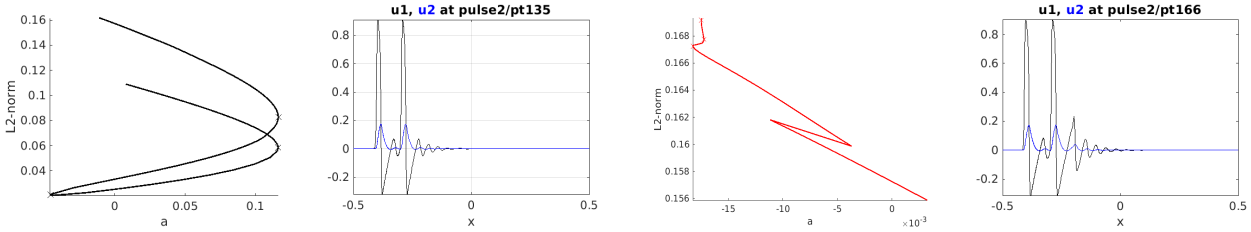

(a) Position in branch after 130 steps (b) $t = 500$, the new starting position (c) New position in branch after 30 steps (d) $t = 0$

Figure 13: Branch jumping setup and emerging of a third pulse

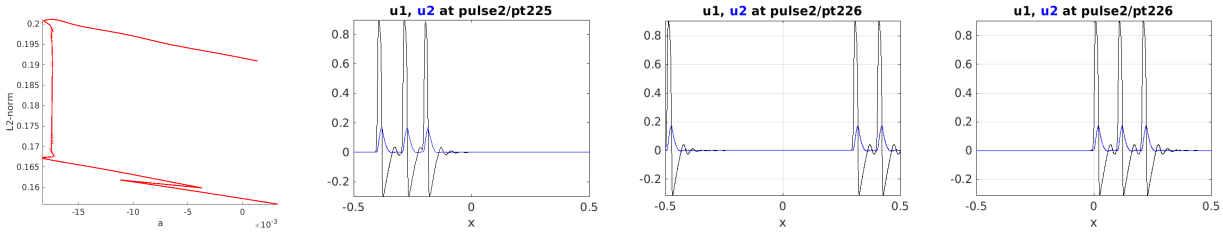

(a) New position in branch after 90 steps (b) $t = 0$ (c) $t = 500$ (d) $t = 1000$

Figure 14: Convergence to a stable 3-pulse

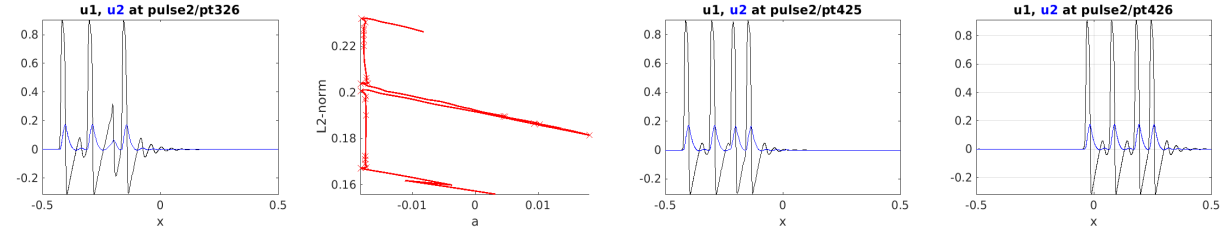

(a) Emerging of the fourth pulse (b) New position in branch after 290 steps (c) $t = 0$ (d) $t = 1000$

Figure 15: Emerging of a fourth pulse and convergence to a stable 4-pulse

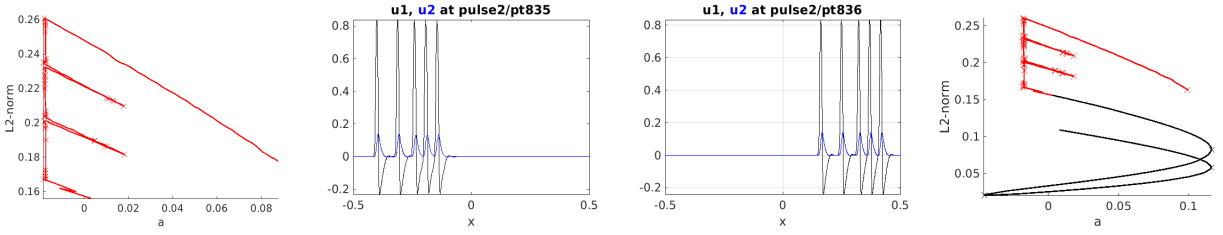

(a) New position in branch after 700 steps (b) $t = 0$ (c) $t = 1000$ (d) Both branches

Figure 16: 5-pulse with convergence

References

[CRS21] Paul Carter, Jens D.M. Rademacher, and Björn Sandstede. Pulse replication and accumulation of eigenvalues. 2021.

[CYS14] Chao-Nien Chen and Choi Y. S. Traveling pulse solutions to fitzhugh–nagumo equations. *Calc. Var. (2015) 54:1–45*, 2014.

[DP22] George Datseris and Ulrich Parlitz. *Nonlinear Dynamics*. Springer, 2022.

[Uec21] Hannes Uecker. *Numerical continuation and bifurcation in Nonlinear PDEs*. SIAM, 2021.